Reprinted from *Proc. 1st International Symposium on Applied Rheology, Korea Jan 18-19, 2001*

FILAMENT STRETCHING RHEOMETRY AND THE EXTENSIONAL VISCOSITY OF DILUTE AND CONCENTRATED POLYMER SOLUTIONS

Gareth H. McKinley[1], Octavia Brauner[1] and Minwu Yao[2]
[1]Massachusetts Institute of Technology, Cambridge, MA 02139
[2]Goodyear Technical Research Center, Akron, Ohio, USA

Introduction

In a plenary presentation at the XIth International Congress in 1992, Ken Walters surveyed some of the recent developments in extensional rheometry of polymer solutions (Walters, 1992). He concluded that experimental results up to that time were 'a disappointment'; and he noted that further international co-operation and input from non-Newtonian fluid dynamics would play important roles in tackling the challenges that still lay ahead in this area of rheology. In the present talk I will update the snapshot of the field captured by Walters, with particular focus on the extensional rheometry of 'mobile' polymer solutions; *i.e.* those that are not viscous enough to be tested in commercial devices such as the Rheometrics Melt Extensiometer (RME) commonly employed for polyolefins and other high viscosity melts (see e.g. Meissner & Hostetler, 1994). The diversity of fluids included in this category is very broad and incorporates dilute and concentrated polymer solutions, inks, adhesives, gels, suspensions, foodstuffs and also lower-viscosity melts such as polycarbonate, Nylon or PET. When viscoelastic filaments are stretched in a filament stretching device they may also exhibit elastically-driven instabilities that lead to complete filament failure, even before the stretching has been completed. At first glance such instabilities may seem to limit the utility of filament stretching rheometers, but additional useful material information can be discerned from the dynamical evolution of the force and radius during the failure event. Such tests may usefully be considered as the functional equivalent of the 'Rheotens' test of spin-line strength for melts (Wagner *et al.* 1996). Two distinctly different modes of filament failure can typically be observed depending on the extent of strain-hardening present in the fluid

Filament stretching devices have their genesis in the work of Matta & Tytus (1990) who suggested using a small cylindrical mass accelerating freely under gravity to stretch a small liquid bridge connecting the mass to a stationary support. Photographic analysis of the rate of decrease in filament radius can then be used to compute an extensional stress growth under the action of a constant force. In the same year, Bazilevsky *et al.* (1990) described a Liquid Filament Microrheometer that may best be summarised as a quantitative version of the 'thumb and forefinger' test we all commonly use to ascertain

the 'stickiness' of a suspicious unknown material! The device imposed a rapid extensional step strain to generate an unstable 'necked' liquid bridge connecting two cylindrical disks which then evolved under the action of viscous, elastic, gravitational and capillary forces. Measuring the time rate of change in the diameter allowed material properties of the test fluid to be quantified. These techniques are examples of a field I shall refer to collectively as *filament stretching rheometry*.

The recent developments in filament rheometry have involved input from across the rheological community and exploited advances in experimental electro-optics, large scale time-dependent numerical calculations, molecular simulations of bead-rod and bead-spring chains in conjunction with constitutive modelling. Utilized jointly, these techniques have enhanced our understanding of the fluid mechanics of such filament stretching experiments, the physics of dilute polymer solutions in strong extensional flows and the dynamics of important extensional flow instabilities that have best been described to date by heuristic rheological concepts such as 'spinnability' and 'tackiness'.

Filament Rheometers

A filament stretching experiment begins with the generation of a long and slender viscoelastic thread. For a slender filament, the velocity field far from the rigid endplates is essentially one-dimensional and extensional in character (Schultz, 1982). Many configurations for generating such flows have been suggested in the literature but, for rheometric purposes at least, two geometries have proved optimal:

- In a filament stretching extensional rheometer (or FISER) a nominally-exponential endplate displacement profile is imposed in order to produce an elongational flow of constant deformation rate, $\dot{\varepsilon}_0$ rather than constant tensile force, as in the original concept of Matta & Tytus. The temporal evolution in the tensile force exerted by the fluid column on the endplate and in the filament radius at the axial midplane of the filament are then measured and used to compute the transient extensional viscosity.

- By contrast, in a capillary breakup extensional rheometer – or CABER for brevity – an extensional step strain of order unity is imposed and the filament subsequently evolves under the influence of capillary pressure without further kinematic input at the boundaries. Large extensional strains can still be attained as the mid-region of the filament progressively necks down and eventually breaks. Typically the only measured quantity is the midpoint radius, $R_{mid}(t)$, of the necking filament.

Both of these experiments can be performed using the same device simply by specifying the total axial strain accumulated before the motion ceases. A typical device is shown below:

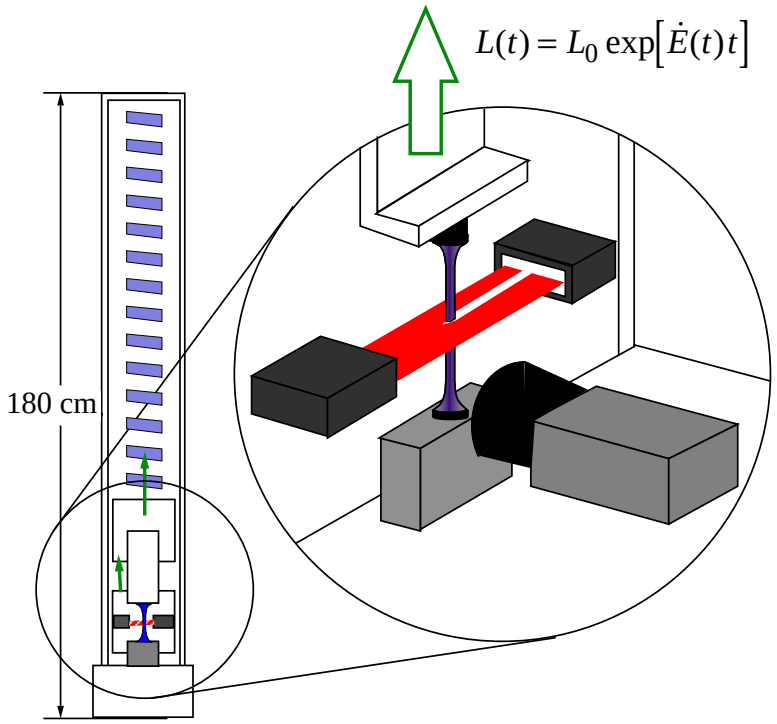

Figure 1: Schematic diagram of the components comprising a typical Filament Stretching Rheometer (FISER).

Kinematics of Filament Stretching Devices

In an ideal homogeneous uniaxial elongational deformation we wish to consider the effects of an irrotational flow on an initially cylindrical fluid element. This potential flow can be represented as

$$v_r = -\tfrac{1}{2}\dot{\varepsilon}_0 r; \qquad v_\theta = 0; \qquad v_z = \dot{\varepsilon}_0 z \tag{1}$$

However in experiments it is not possible to realize such a configuration. At small strains, the no-slip condition arising from the rigid end fixtures leads to a 'reverse squeeze flow'. Since the stress in a dilute polymer solution is carried primarily by the solvent for small strains, this flow can be considered analytically using a lubrication analysis (Spiegelberg *et al.* 1996) and the strain rate of material elements near the middle of the filament is found to be 50% larger than the value based on the rate of separation of the endplates; $\dot{\varepsilon}_0 = 1.5\dot{\varepsilon}_L$. At larger strains, $\varepsilon \geq 2$, simulations and experiments show that strain-hardening significantly affects the rate of evolution in the mid-filament diameter of a viscoelastic fluid.

Numerical simulations show that the principal advantage of a filament stretching experiment is that the measurements of force and midpoint radius always correspond to observations of the constitutive response of the *same* Lagrangian fluid element; *i.e.* the element located at the axial midplane of the elongating filament. This is in contrast to other techniques such as a Spinline Rheometer in which a single integrated measurement of the total tension is used to characterize the spatially unsteady kinematics experienced by material elements as they traverse the spin-line.

The simplest approach is to impose an ideal exponential stretching deformation at the end plate of the form $L_p(t) = \exp\left[\dot{E}\, t\right]$ however this does NOT result in a homogeneous elongation of the fluid sample due to the no-slip conditions discussed above. The instantaneous deformation rate experienced by the Lagrangian fluid element at the axial midplane can be determined in a filament rheometer in real-time using a high resolution laser micrometer that measures $R_{mid}(t)$ and using the relationship

$$\dot{\varepsilon}_{mid}(t) = \frac{-2v_r(r = R_{mid})}{R_{mid}} = \frac{-2}{R_{mid}} \frac{dR_{mid}}{dt} \tag{2}$$

The Hencky strain accumulated by the midpoint element can be found by direct integration of eq. (2) to give

$$\varepsilon = \int_0^t \dot{\varepsilon}(t')\ \mathrm{d}t' = 2\ln\left(R_0 / R_{mid}(t)\right). \tag{3}$$

This type of experiment is referred to as a Type II experiment using the nomenclature of Kolte, Szabo & Hassager (1997). However, to explore more precisely the actual constitutive response of a fluid it is necessary to decouple the kinematics from the resulting evolution in the polymeric stresses so that the appropriate constitutive equation can be directly integrated. It is thus essential to impose a constant rate of deformation:

$$\dot{\varepsilon}_0 = -\frac{2}{R_{mid}} \frac{\mathrm{d}\, R_{mid}(t)}{\mathrm{d}\, t} = -2 \frac{\mathrm{d}\, \ln\left(R_{mid}(t)/R_0\right)}{\mathrm{d}\, t}, \tag{4}$$

This is referred to as a Type III experiment and the goal of kinematic control in a FISER can thus be stated in the form:

Find the form of $L_p(t)$ such that $\dot{\varepsilon}_{mid}(t) = \dot{\varepsilon}_0$ for all times $t \geq 0$

The Deborah number resulting from such an experiment is constant and given by $De = \lambda \dot{\varepsilon}_0$ where λ generically denotes the longest (model-dependent) relaxation time of the test fluid.

In their groundbreaking paper, Tirtaatmadja & Sridhar (1993) used an iterative approach to finding the required endplate displacement profile, $\dot{L}_p(t)$. More recently open and closed-loop control strategies have been considered which considerably simplify the task of the experimentalist (Orr & Sridhar, 1999; Anna *et al.* 1999). Numerous experimental FISER variants have been developed, and by precisely controlling this endplate displacement profile it is now possible to reliably attain the desired kinematics. The results can be best represented on a "Master Curve" showing the evolution of the *imposed* axial strain $\varepsilon_L = \ln\left(L_p(t)/L_0\right)$ vs. the *resulting* radial Hencky strain at the midplane: $\varepsilon_{mid} = -2\ln\left(R_{mid}(t)/R_0\right)$. Very recent computational rheometry analysis shows that this approach is well-posed for a number of different constitutive models. Sample Type II calculations (ideal exponential axial stretching)are shown below in Figure 2 for the Newtonian, Oldroyd and Giesekus models. For an

ideal uniaxial elongation the two strain measures are the same such that $\varepsilon_L = \varepsilon_{mid}$, whereas for the lubrication solution $\varepsilon_L = \frac{2}{3}\varepsilon_{mid}$.

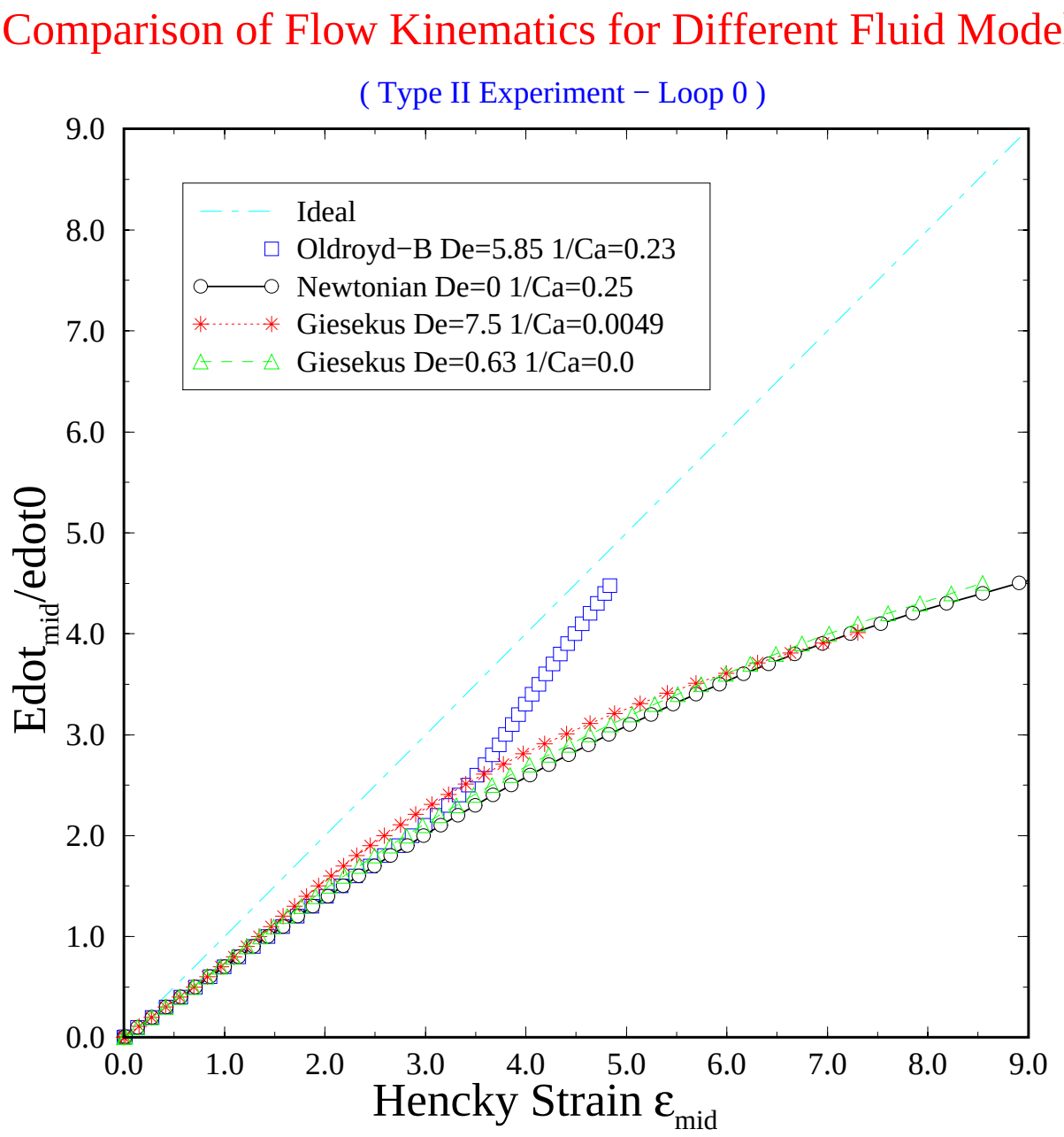

Fig..2 Master curve of axial and radial strain measures numerically computed for different constitutive models over a range of Deborah and capillary numbers.

Close inspection of Fig 2 shows that ALL viscoelastic fluid models initially follow this lubrication solution since the viscoelastic stresses are negligible at short times. At long times and larger

strains however the different constitutive models predict very different evolution in the master curve profiles. For strongly strain-hardening fluids (e.g. the Oldroyd-B model which describes dilute polymer solutions such as ideal elastic Boger fluids) the curve eventually approaches the ideal limit corresponding to uniaxial elongation of a cylinder. However for a weakly strain hardening material (e.g. the Giesekus model which describes entangled materials such as concentrated solutions or melts) the curves progressively diverge from the ideal case. This is a result of a viscoelastic necking instability which is currently of great interest both experimentally and theoretically since it is related to concepts of melt strength and' spinnability'.

An analogous master curve is shown below for a concentrated polystyrene solution consisting of 12 wt% monodisperse polystyrene (M_w = 2x10^6 g/mol.) dissolved in TCP.

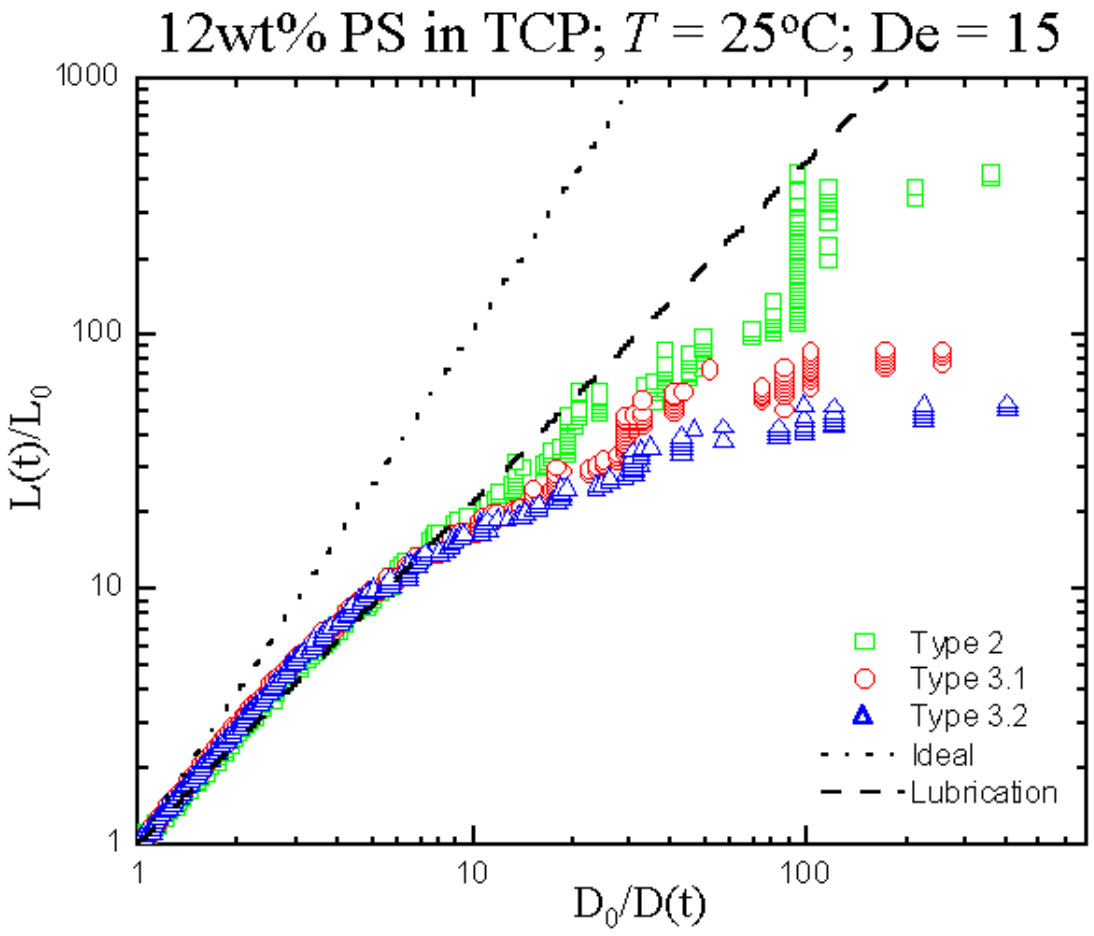

Fig. 3 Convergence of the master curve of axial and radial strain measures for 12 wt% entangled polystyrene experimentally measured in consecutive tests.

This fluid has been characterized by Venerus and co-workers and is moderately entangled with $M_w/M_e \approx 10$ and a (longest) reptation time $\lambda \equiv \tau_d \approx 15$ s. For such weakly strain-hardening fluids our

numerical calculations and experimental tests show that it is necessary to below multiple iterations in order to converge on a final master curve. The output $R_{mid}^{[j]}(t)$ from the *j*-th test is used in conjunction with the master curve to provide the input data $L^{[j+1]}(t)$ for the next test. The successive evolution of the resulting master curve is shown in figure 3.

Experimental Results

The experimental observables in a filament stretching experiment include the global evolution in the axial profile of the filament $R(z,t)$, the midpoint radius $R_{mid}(t)$, and the tensile force on the endplate $F_z(t)$. The evolution in the force is typically non-monotonic, showing an initial, solvent-dominated peak at early times, followed by strain-hardening and, possibly, a second maximum at large strains after the extensional stresses saturate and the extensional viscosity of the fluid reaches its steady-state value. A complete analysis of the appropriate force balance for the filament is given by Szabo [19]. After removing contributions from surface tension, gravity and inertia, the transient uniaxial extensional viscosity is given by

$$\eta_E^{+}(\dot{\varepsilon}_0,t) \equiv \frac{F_z(t)}{\pi R_{mid}(t)^2 \dot{\varepsilon}_0} \quad . \tag{5}$$

A sample force profile for a dilute polymer solution is shown below. This ideal elastic fluid is part of a homologous series studied by Anna et al. (2001) in an international 'round-robin' comparison of filament stretching devices. At short times ($\varepsilon < 2$) the stress in the fluid is carried entirely by the viscous oligomeric solvent and the filament profile is that of a concave liquid bridge (see also Yao et al. 1998). At intermediate times ($2 \le \varepsilon \le 4$) significant strain-hardening is observed. At larger times the force goes through a maximum as the stress begins to saturate until ultimately the fluid undergoes an elastic instability at a critical strain $\varepsilon_{crit} \approx 5.1 \pm 0.1$. This peeling instability leads to a significant 'spike' in the force profile and the onset of a symmetry breaking transition leading to the formation of elastic fibrils (Spiegelberg & McKinley, 1997; Ferguson et al. 1998). For comparison, the evolution in the force profiles in the entangled concentrated PS solution are shown as a function of deformation rates in Figure 5.

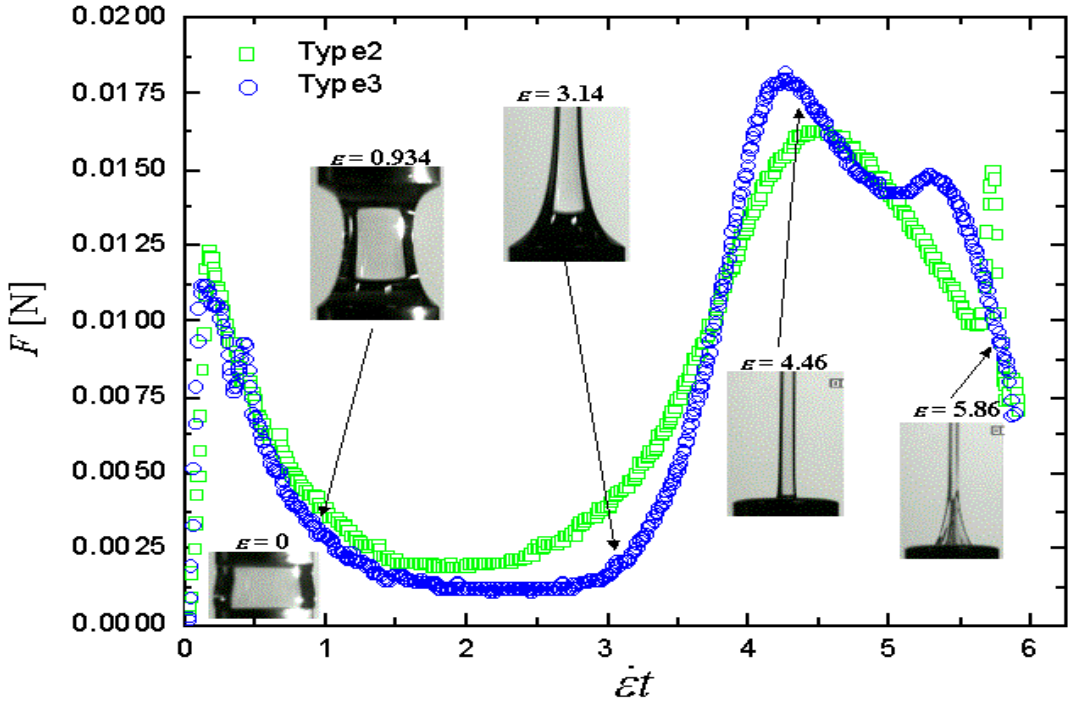

Fig. 4 Evolution in the tensile force curve and axial filament profile in Type II and Type III elongational stretching experiments for a dilute polystyrene Boger fluid.

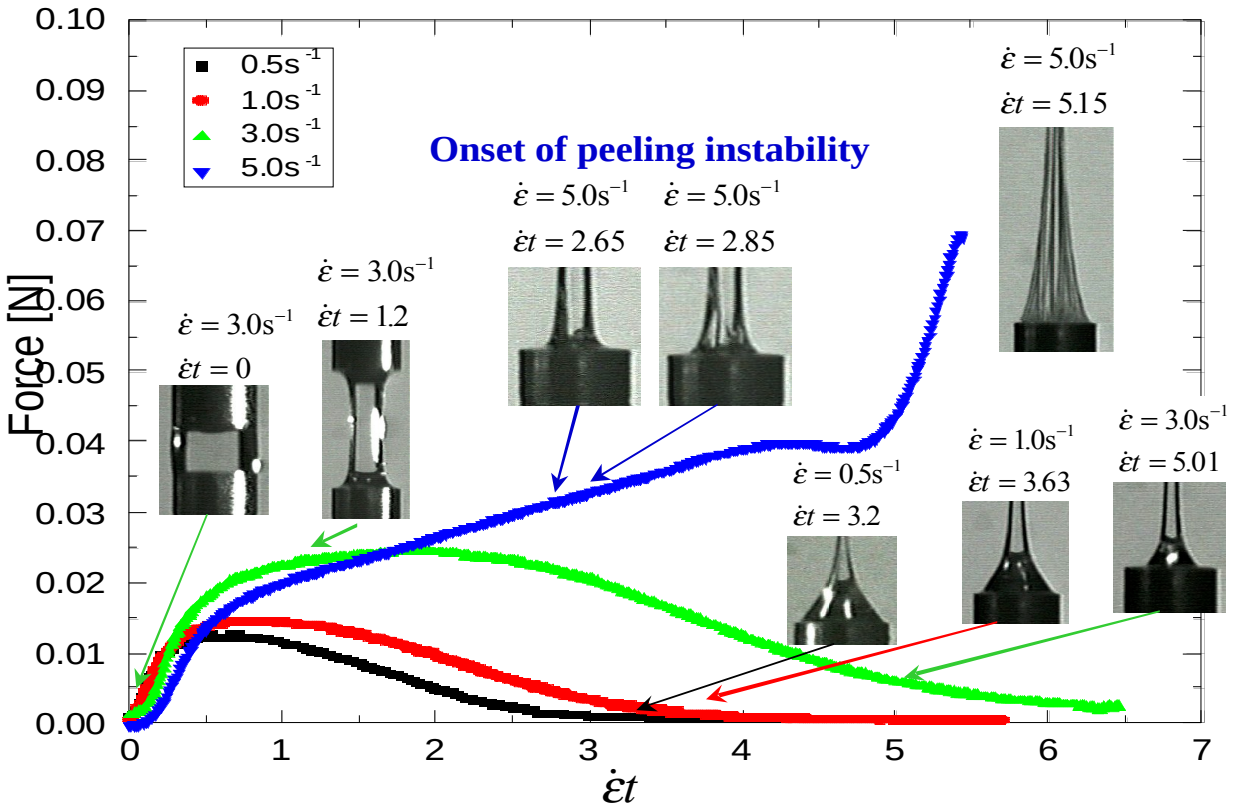

Fig. 5 Evolution in the tensile force curve and filament profile for a weakly strain-hardening entangled polystyrene fluid

In entangled solutions it is essential to recognize that there are several important characteristic polymeric time scales, including the reptation time (typically denoted τ_d) for the tubes and the Rouse time for chain stretching(denoted τ_R) within the tube (Doi & Edwards, 1986). At low deformation rates $\tau_d^{-1} \le \dot{\varepsilon}_0 < \tau_R^{-1}$ the fluid is only weakly strain-hardening as the confining tube is oriented with the flow but the chain itself remains relaxed at close to its equilibrium length within the tube. In this case the force in the filament passes through a maximum and ultimately decays at large strains as the radius at the midplane exponentially decays. In this case the filament does not show a peeling instability but instead a 'necking' instability close to the midplane. This necking instability has also been considered theoretically (Ide & White 1976; Olagunju, 1999) and numerically (Yao et al. 2000). However, at higher deformation rates $\tau_R^{-1} \le \frac{1}{2}\dot{\varepsilon}_0$ constitutive models such as the Doi-Edwards-Marrucci-Grizutti (DEMG) model show that chain stretching can occur and consequently extensive strain-hardening in the elongational viscosity is observed. This results in the endplate peeling observed at the imposed strain rate of $\dot{\varepsilon}_0$=5 s^{-1} in Figure 5 above. From the critical conditions for onset of peeling, we can thus estimate that $\tau_R \approx 0.13 \pm 0.03$ s. It is also worth noticing that because of the lower extensibility of the entangled chains ($L^2_{\text{entangled}} \sim M_e$ cf. $L^2_{dilute} \sim M_w$) the onset of peeling occurs at a significantly lower Hencky strain.

Despite the onset of the necking instability at low strain rates and the elastic peeling instability at large strain-rates, filament stretching devices can still be used to extract the transient elongational viscosity function $\eta_E^+(\dot{\varepsilon}_0, t)$ provided that the master curve methodology described above is utilized to realize an ideal 'Type III' master curve. The evolution in the Trouton ratio for the concentrated polymer solution is shown below in Figure 6

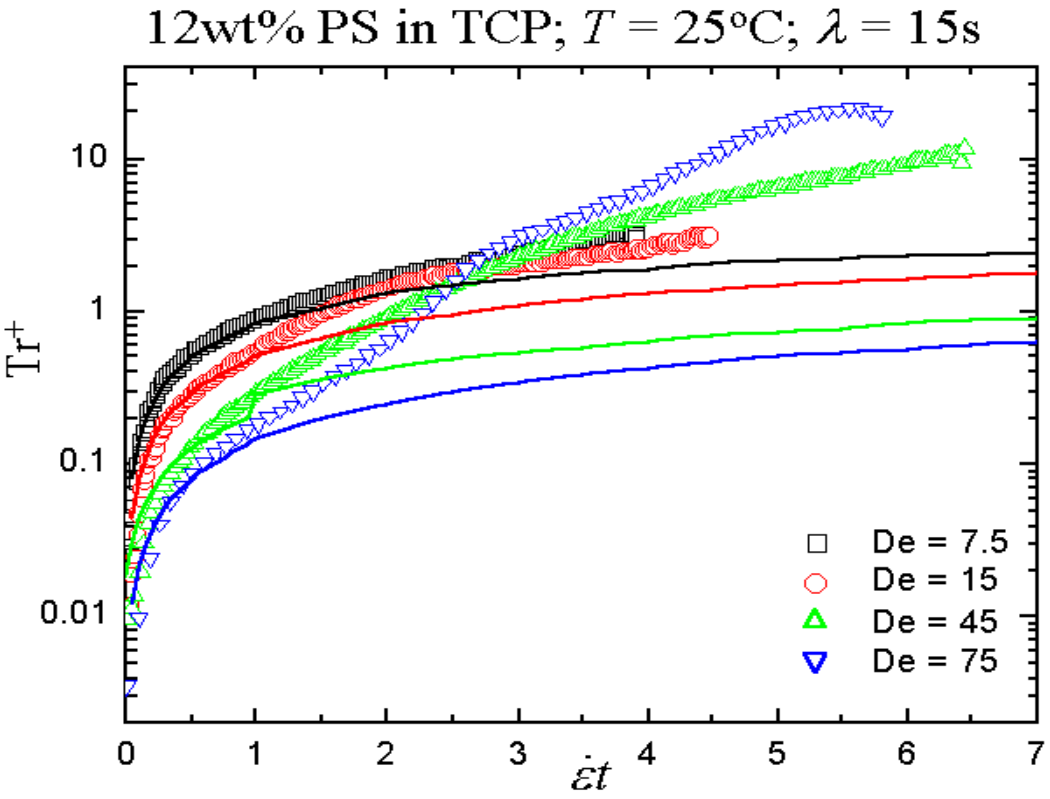

Fig. 6 Transient extensional viscosity for the 12 wt% entangle PS fluid as a function of stretch rate.

The solid lines in Figure 6 show the results expected from linear viscoelastic theory which gives

$$Tr^{+} \equiv \frac{\eta_E{}^{+}}{\eta_0} = \frac{1}{\eta_0}\sum_{i=1}^{n} 3\eta_j\left(1-\exp(-t/\lambda_j)\right) = \frac{1}{\eta_0}\sum_{i=1}^{n} 3\eta_j\left(1-\exp\left(-\dot{\varepsilon}_0\, t/(\lambda_j\dot{\varepsilon}_0)\right)\right) \qquad (6)$$

where we have indicated explicitly in the last expression that since it is typical to plot the Trouton ratio vs. the total Hencky strain $\varepsilon = \dot{\varepsilon}_0 t$, the linear viscoelastic predictions do vary with $\dot{\varepsilon}_0$. We have used a 9 mode discrete spectrum of relaxation modes $\{\eta_j, \lambda_j\}$ reported by Venerus and co-workers with no adjustments. At small strains it is clear that we can recover the linear viscoelastic envelope before strain-hardening develops at higher strains and strain rates.

Conclusions

The number of materials tested in filament stretching devices continues to expand and now includes a number of dilute and semi-dilute 'Boger' fluids, entangled polymer solutions and melts and also liquid crystalline solutions. It seems fair to say that filament stretching results now form a standard component of the suite of tests used to characterise many polymer solutions and other complex fluids.

Much work remains to be done in theoretically understanding the onset of the elastic instabilities that occur at large strains; however additional information about the extensional rheology of the material is encoded in these responses and deserves detailed analysis. Future advances in this area will no doubt result from the same elements that have so benefited the first decade of filament stretching rheometry; a strong interplay between experiment, numerical simulation and kinetic theory, together with a spirit of international collaboration.

Acknowledgments

This work has been supported in part by grants from the Lord Corporation, DuPont Educational Aid Foundation, and NASA through grant NCC3-610.

BIBLIOGRAPHY

S.L. Anna, C.B. Rogers and G.H. McKinley, *J. Non-Newt. Fluid. Mech.* (1999) 87 307-335.

S.L. Anna, G.H. McKinley, D.A. Nguyen, T. Sridhar, S.J. Muller, J. Huang and D.F. James, *J. Rheol.* (to appear Jan/Feb 2001).

A.V. Bazilevsky, V.M. Entov and A.N. Rozhkov, in "*Third European Rheology Conference*", (*Ed.* D.R. Oliver) Elsevier Applied Science, (1990), 41-43.

Doi, M. and Edwards, S.F., The Theory of Polymer Dynamics, OUP, Oxford, 1986.

J. Ferguson, B. Reilly and N. Granville, *Polymer* (1997) 38 795-800

Ide, Y. and White, J.L., *J. Appl. Polym. Sci.*, **20**, (1976), 2511-2531.

M.I. Kolte, H.K. Rasmussen and O. Hassager, *Rheol. Acta* (1997) 36 285-302.

J.E. Matta and R.P. Tytus, *J. Non-Newtonian Fluid Mech.* (1990) 35 215-229.

J. Meissner and J. Hostettler, *Rheol. Acta* (1994) 33 1-21.

D. O. Olagunju, *J. Non-Newt. Fluid Mech.*, **87**(1), (1999), 27-46.

N.V. Orr and T. Sridhar, *J. Non-Newt. Fluid Mech.* (1999) 82 203-222.

W.W. Schultz, *J. Rheol.* (1982) 26 331-345.

S.H. Spiegelberg, D.C. Ables and G.H. McKinley, *J. Non-Newt. Fluid Mech.* (1996) 64 229-267.

S.H. Spiegelberg and G.H. McKinley, *J. Non-Newt. Fluid Mech.* (1996) 67 49-76.

P. Szabo, *Rheol. Acta* (1997) 36 277-284.

V. Tirtaatmadja and T. Sridhar, *J. Rheol.* (1993) 37 1081-1102.

M.H. Wagner, V. Schulze and A. Göttfert, *Polym. Eng. Sci.* (1996) 36 925-935.

K. Walters, in "*Theoretical and Applied Rheology*", Vol. 1, (Ed. P. Moldenaers and R. Keunings) Elsevier, Brussels (1992), 16-23.

M. Yao, G.H. McKinley and B. Debbaut, *J. Non-Newt. Fluid Mech.* (1998) 79 469-501.

M. Yao and G.H. McKinley, *J. Non-Newt. Fluid Mech.* (1998) 74 47-88.